Cascaded boost converter-based high-voltage pulse generator for pulsed electric field applications

S. Krishnaveni [ID], **V. Rajini**

Sri Sivasubramaniya Nadar College of Engineering
India
e-mail: {krishnavenis/rajiniv}@ssn.edu.in

Abstract: Food processing technologies for food preservation have been in constant development over a few decades in order to meet current consumer's demands. Healthy competitive improvements are observed in both thermal and non-thermal food processing technology since past two decades due to technical revolution. Among these novel technologies, pulsed electric field food processing technology has shown to be a potential non-thermal treatment capable of preserving liquid foods. The high-voltage pulse generators specifically find their applications in pulsed electric field technology. So, this paper proposes a new structure of a high-voltage pulse generator with a cascaded boost converter topology. The choice of a cascaded boost converter helps in selecting low DC input voltage and hence the size and space requirement of the high-voltage pulse generator is minimized. The proposed circuit is capable of producing high-voltage pulses with flexibility of an adjusting duty ratio and frequency. The designed circuit generates a maximum peak voltage of 1 kV in the frequency range of 7.5–20 kHz and the pulse width range of 0.8–1.8 μs. Also, the impedance matching between the cascaded boost converter and the high-voltage pulse generator is found simple without further additional components. The efficiency can be improved in the circuit by avoiding low frequency transformers.

Key words: cascaded boost converter, food processing, high-voltage pulse, MOSFET, pulsed electric field

1. Introduction

The commonly known traditional food processing methods like cooking, heating, freezing, refrigeration and blanching are preferred by people at their homes. However, from a large-scale view, the food processing industries combine these techniques with other processing operations

with the help of different technical prospects that could not be commonly practiced by consumers during house-hold processing.

The modern technologies include high-temperature short-time heating or vacuum heating, high pressure treatment, extrusion and microwave processing. These methods usually emphasize on food preservation with maximum retention of food quality [1–4]. So, non-thermal food processing methods have gained attention of researchers as a substitution of traditional thermal processing methods of food. Among the non-thermal processes, pulsed electric field [PEF] technology offers low processing temperature, efficient energy utilization, retaining the food quality like flavor, colour, taste and nutrients [5–11]. Moreover, the generation of high-voltage pulses requires a pulsed voltage generator as an inevitable part of the PEF food processing.

A commercial electroporator is capable of providing high electric field intensity in the order of 10 kV/cm–100 kV/cm but it is found feeble in the study of microbial inactivation by PEF technology due to the bigger size of the high-voltage pulse generator [12]. Whenever the voltage across the microbe's outer membrane (known as transmembrane voltage) reaches $\cong$ 1 V by the applications of the high-voltage pulses, the microbe gets inactivated [13]. This phenomenon known as electroporation is majorly influenced by either pulse magnitude or the number of pulses applied [14]. It is proven from the literature that electrical parameters are interrelated in determining the efficiency of the microbial inactivation [15–17]. The PEF generator can be developed based on either higher output voltage at lower frequency or higher frequency at lower voltage in the range of 1 kV to 5 kV [18]. Generally, the PEF generator design should have high effectiveness, portable, cost-effective and flexible circuit design for food processing in order to increase the effectiveness of the PEF technology.

PEF generators can be designed by using advanced semiconductor devices to reduce the size and space requirement unlike the conventional PEF generators discussed in [19–21] and the individual PEF generator developed in the past two decades that possesses its own advantages and disadvantage. In conventional PEF generators, the thyratron, ignitron, gas spark gaps and trigatron are used as switching elements. But, the classical switches have the drawbacks such as: the repetition rate is limited (less than 100 Hz), the complex triggering circuit design and the switching time delays which try to alter the wave-shape. But, the embellished technological improvements in semiconductor technology have been brought in PEF systems to make them efficient [18,22–26]. This paper proposes a high-voltage pulse generator that focuses on reducing the input DC voltage requirement for the high-voltage pulse generation by selecting cascaded boost converter topology as a front-end converter. The cascaded boost converter increases the low-input DC voltage to high-voltage and consists of power electronics semiconductor switches. The choice of power electronic switches minimizes the size of the equipment and also improves the reliability of the circuit. The proposed circuit is designed to generate high-voltage pulses of a maximum peak of 1 kV with an adjustable pulse width in the range of 0.8–1.8 μs and a frequency range of a few kHz–50 kHz. The following sections elaborate the design and the experimental results obtained in detail.

2. Electric circuitry and design

A high-voltage pulse generator requires high-voltage DC supply as an input side source. There are many conventional methods available such as rectifier circuits, voltage doubler circuits and voltage multiplier circuits. One of the simplest methods is to use rectifier circuits, either a

half-wave rectifier or a full-wave rectifier. However, these circuits also require high AC voltage as input. Again, several units are to be connected in series as the voltage demand increases. When a number of units are used in series, transient voltage distribution across each unit becomes non-uniform and special care must be taken to make the distribution uniform. Moreover, the circuits need large supply and an isolation transformer. So, the proposed generator has been designed in a non-isolated manner to avoid the huge transformers with the help of power electronics DC-DC converters. Though there are many topologies that have been developed to increase the voltage level like a multiplier, switched capacitor and multilevel converters, the cascaded boost converter is selected in the present work. The cascaded boost converter is a straight forward approach to increase the voltage gain in geometric progression with reduced components and without any complicated circuit connection. So, the proposed circuit in this paper avoids such a huge isolating transformer by the selection of the cascaded boost converter and the respective circuit is shown in Fig. 1. This helps in reducing the input voltage and the space requirement.
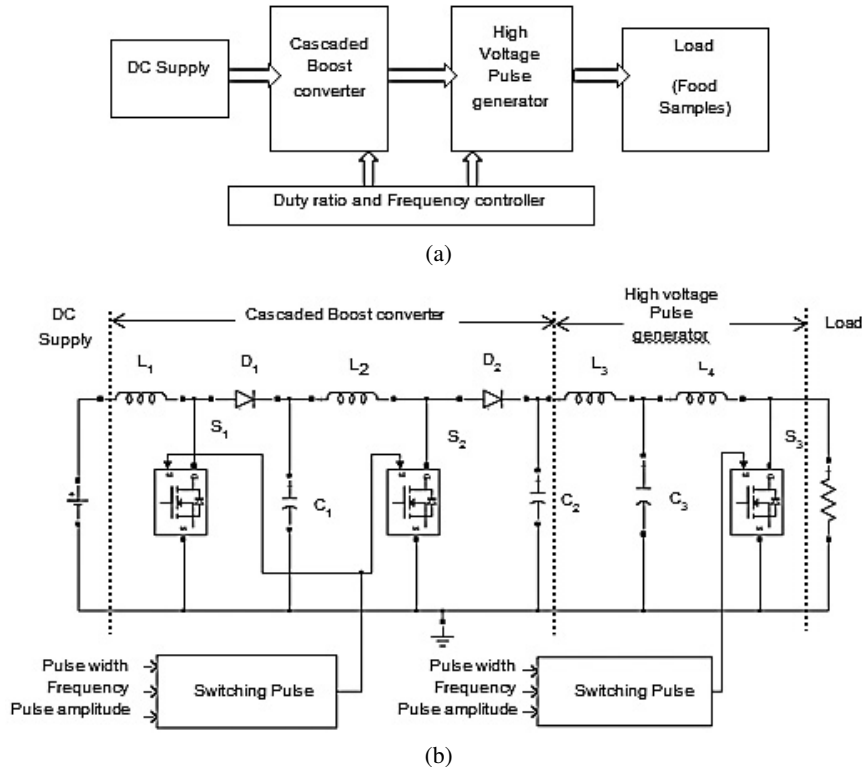
(a)

(b)

Fig. 1. High-voltage pulse generator: (a) block diagram; (b) circuit diagram

2.1. DC power supply

A 48 V battery is used to feed the cascaded boost converter. This can be replaced by two 24 V, 25 A switched mode power supply (SMPS) connected in series.

2.2. Cascaded boost converter

The cascaded boost converter has a better voltage gain than the conventional boost converter and so, the proposed high-voltage pulse generator is designed based on the cascaded boost converter [27, 28]. The cascaded boost converter is as shown in Fig. 1 and this circuit results from the association of two identical elementary boost converters connected in tandem. It consists of an input voltage source, two independently controlled switches S_1, S_2, two freewheeling diodes D_1, D_2, two capacitors C_1, C_2 and two inductors L_1 and L_2 [29, 30]. The modes of operation are as follows.

Mode 1: This begins when the switch S_1 is turned on. During this period, S_2 will remain off. The inductor L_1 gets loaded through the supply voltage and stores the energy. This mode finishes when S_1 is turned off.

Mode 2: During this mode of operation, S_1 is turned off and S_2 is turned on. The output of the first stage has now become the input of the second stage. The inductor L_2 gets loaded through the supply voltage and stores the energy. This mode of operation is finished when S_2 is turned off.

The voltage ratio is calculated by using Equation (1) as follows [31–33]:

$$\frac{V_{\text{out}}}{V_{\text{in}}} = \frac{1}{(1 - D_1)} \frac{1}{(1 - D_2)}, \tag{1}$$

where D_1 is the duty cycle of the first stage and D_2 is the duty cycle of the second stage in the cascaded boost converter circuit.

The output and inductor currents are given by the following Equations (2)–(4).

$$I_{\text{out}} = \frac{V_{\text{out}}}{R}, \tag{2}$$

$$I_{L_2} = \frac{I_{\text{out}}}{1 - D_2}, \tag{3}$$

$$I_{L_1} = \frac{I_{L2}}{1 - D_1}, \tag{4}$$

where I_{L_1} and I_{L_2} are the currents flowing through the inductors L_1 and L_2, respectively. The inductor and capacitor values can be calculated by using the following Equations (5)–(8).

$$L_1 = \frac{D_1 V_{\text{in}}}{f \Delta i_{L1}}, \tag{5}$$

$$L_2 = \frac{D_2 V_{\text{in}}}{f \Delta i_{L2}}, \tag{6}$$

$$C_1 = \frac{D_1 V_1}{f R \Delta V_{C1}}, \tag{7}$$

$$C_2 = \frac{D_2 V_{\text{out}}}{f R \Delta V_{C2}}, \tag{8}$$

where V_1 and V_2 are the voltage across the capacitors C_1 as C_2, respectively.

Based on the requirement, the circuit components are chosen in order to produce high-voltage pulses of peak 1.7 kV and the values are tabulated in Table 1.

Table 1. Circuit components.

Component	L_1	L_2	C_1	C_2	L_3	L_4	C_3
	1 mH	1 mH	10 μF	10 μF	220 μH	220 μH	10 μF
Switches	S_1 IXTX20N247, 20 A, 1500 V			S_2 IXTX20N247, 20 A, 1500 V		S_3 IXTX20N247, 20 A, 1500 V	
Duty ratio	0.66			0.66		0.5	
Switching frequency	Maximum – 50 kHz			Maximum – 50 kHz		Maximum – 50 kHz	

Fig. 2 shows the simulation results of the circuit using MATLAB/SIMULINK. Fig. 2(a) illustrates the waveform of the input voltage and the current, where the input current varies as the load changes its value. So, the maximum current drawn from the input side supply is determined by the capacity of the battery. Fig. 2(b) represents the waveforms of output electrical signals at the second stage of the cascaded boost converter. When the steady state is achieved, the voltage is maintained as constant at 400 V and the current I_{L_2} attains 12 A.
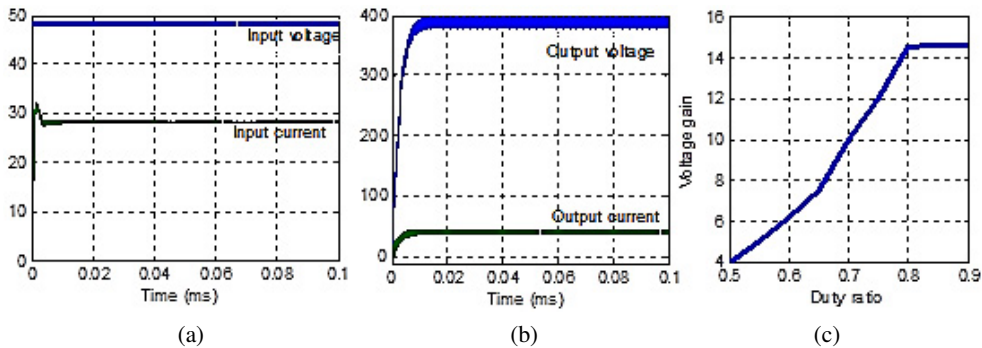

Fig. 2. (a) input voltage and current; (b) output voltage and current; (c) duty ratio vs. voltage gain

It is observed that the ripple content in the input current and the inductor current I_{L2} are very low. The voltage gain increases when the duty cycle increases as in other power converters and the corresponding plot is shown in Fig. 2(c). It is observed that the pulse voltage is increased with the increased load resistance.

2.3. High-voltage pulse generator

The cascaded boost converter output acts as the input to the high-voltage pulse generator. The cascaded boost converter is connected to the next stage of the high-voltage pulse generator with proper impedance matching through the inductor L_3 which is considered an impedance matching device. The value of the L_3 inductor should be selected in such a way that the variations in load should not be reflected in the DC supply on the input side. So, the selection of the cascaded boost converter as a front-end converter simplifies the impedance matching between

the cascaded boost converter and the high-voltage pulse generator. The high-voltage pulses are generated whenever the current through the inductor L_4 is interrupted at regular intervals with the help of the MOSFET switch S_3 in the circuit. The current through the inductor L_4 is calculated by using following Equation (9).

$$I_{L_4}(t) = \frac{1}{L_4} \int V_{L4}(t)\,\mathrm{d}(t),$$ (9)

$$L_3 \text{ or } L_4 = \frac{V_{L4} \times T_{\mathrm{on}}}{I_{L4,\mathrm{peak}}},$$ (10)

$$C_3 = \frac{I_{L4} \times T_{\mathrm{on}}}{V_{L4}},$$ (11)

where T_{on} is the switch-on time period of MOSFET S_3.

The output voltage and current pulse generated by the proposed circuit are shown in Fig. 3 for a load resistance of 50 Ω, which is the typical value of the biological load (food samples) [34], and the duty ratio is set as 0.65 at 20 kHz. The load current also follows the pulse pattern which is recommended by the biological load, where the heat generated during the process should be maintained as low as possible. The steep pulses are determined by the rise/fall time characteristics of the MOSFET switch used in the circuit. The pulse energy can be stored and then delivered to the food samples.
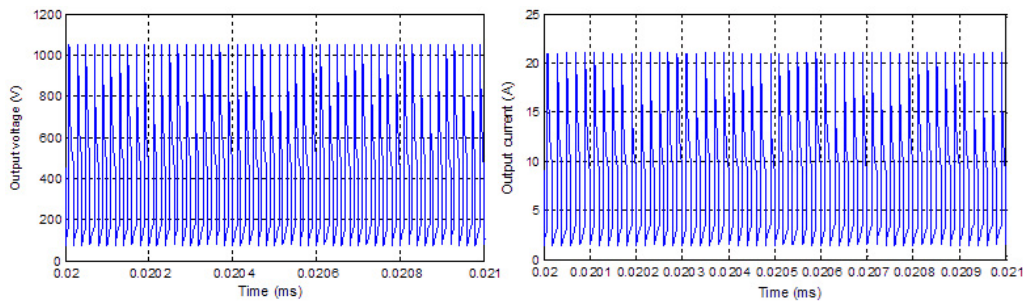

Fig. 3. Output pulse voltage and current duty ratio 0.65 at 20 kHz

3. Experimental results

The proposed circuit is designed to work in open loop mode and fabricated. Pulse width modulation technique is used to adjust the pulse width and pulse frequency. A PIC18F2550 microcontroller is programmed in such a way to adjust the frequency and pulse width in the designed topology. PIC18F2550 is energized by a 5 V DC supply which is built by using a bridge rectifier (diode 1N4007) along with a voltage regulator (IC 7805). A maximum frequency of 50 kHz and 75% of a duty ratio are obtained by changing the output ports of PIC18F2550. The voltages and current of the proposed converter are different at different stages. The voltage at the first stage of the cascaded boost converter is doubled at the end of the second stage of the

cascaded boost converter. The MOSFET switches are identically selected based on the maximum voltage of the circuit. So, three identical MOSFETs, IXTX20N247, 20 A, 1500 V, are used in the proto type pulse generator by considering the safety margin, and moreover, the MOSFETs are inexpensive. But, the MOSFETs and other components should be perfectly selected as per the design, if the output voltage range is extended further. The experimental set up is shown in Fig. 4. The input side battery is replaced by a series-connected SMPS of 24 V rating each. The food chamber, which is made up of acrylic glass, is used to carry a liquid food sample of volume 100 ml.
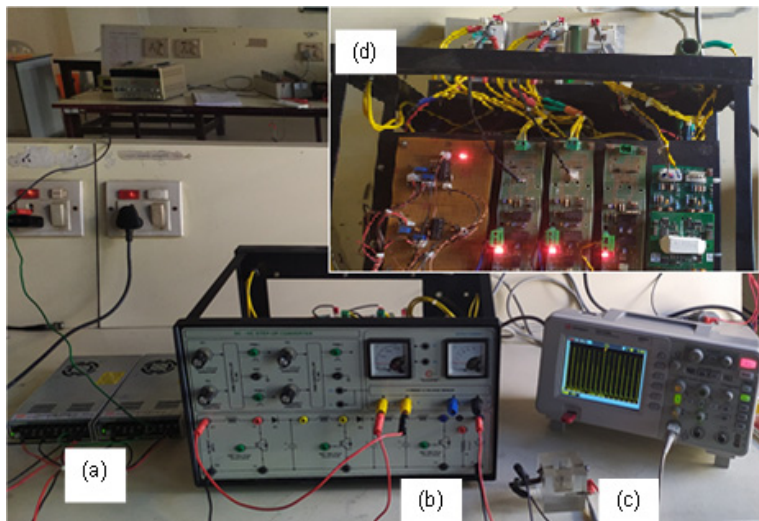

Fig. 4. Experimental set up: (a) DC power supply; (b) front panel of the fabricated circuit; (c) food chamber; (d) internal circuit

The fabricated circuit is tested for two different input voltage (24 V and 48 V), different frequencies and pulse widths for a resistive type load of 50 Ω, and the results are tabulated in Table 2. It is observed that the output pulse magnitude is found maximum when the frequency is set at 7.5 to 20 kHz when the duty ratio is 0.5. The output pulse width is found in the range of 0.8–1.78 μs, and it can be achieved by adjusting the switching pulse width of the MOSFET switch S_3.

In the proposed circuit, separate driving circuits are preferred to trigger the MOSFET switches S_1, S_2 and S_3. The output pulse magnitude is doubled whenever the input DC voltage doubles. The designed cascaded boost converter works in continuous mode, and so it helps to provide like a constant DC source to the high-voltage pulse generator.

Fig. 5 shows the output voltage pulse and looks similar to the simulation output. The voltage peak is basically determined by the di/dt rating of the inductors (L_3 and L_4) used. The desired value of the output voltage can be determined by the properties of liquid food samples and the volume selected for the experiments. The voltage peak values can be adjusted by switching frequency and a duty ratio. The proposed circuit has the reliability for the maximum voltage under

Table 2. Experimental results of the prototype high-voltage pulse generator.

Input voltage (V)	Input current (A)	Frequency (kHz)	Switching pulse width (μs)	Duty ratio	Output voltage, peak (V) pulse width (μs)
48	3	50	10	0.5	520, 1.55
	1.5		5	0.25	210, 1.78
	3.6	20	20	0.5	1000, 0.81
	2		10	0.25	500, 1
	4	15	24	0.32	1000, 0.84
	2.5		12	0.2	500, 1.16
	3.6	10	21	0.21	1000, 0.81
	2		11	0.11	500, 1
	3	7.5	20	0.16	1000, 0.81
	2		10	0.08	500, 1
24	3	50	10	0.5	215, 1.55
	1.5		5	0.25	106, 1.78
	4	20	24	0.5	500, 1.03
	2		12	0.25	250, 1.38
	2.5	15	24	0.4	500, 1.01
	2		12	0.25	250, 1.38
	2	10	25	0.28	520, 1.03
	1.5		13	0.28	250, 1.38
	2	7.5	29	0.22	500, 1
	1.5		15	0.11	250, 1.4

both the control parameters of switching frequency and a duty ratio. The maximum output current is observed as 250 mA for the developed prototype. For a 1 kV output voltage pulse, the average output voltage is found to be 500 V and so, the overall maximum efficiency is found at 87%. Though the cascaded boost converter increases the number of components when compared to the front-end rectifier in the conventional topology, the circuit avoids low-frequency transformers and so, the efficiency is found better for the proposed topology.
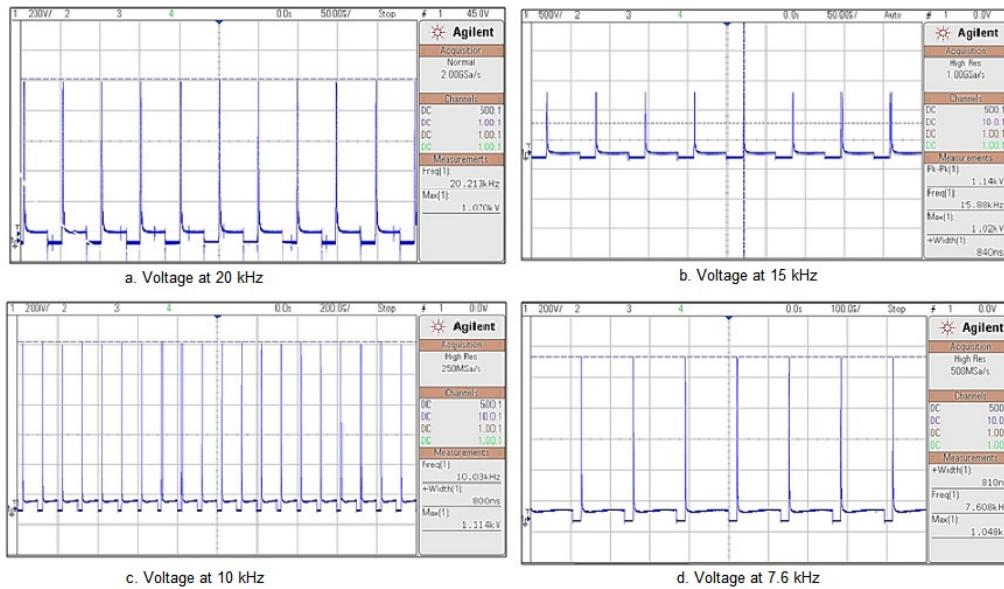
a. Voltage at 20 kHz

b. Voltage at 15 kHz

c. Voltage at 10 kHz

d. Voltage at 7.6 kHz

Fig. 5. Output voltage pulses for a resistive load of 50 Ω

4. Conclusions

The proposed circuit has no step-up low-frequency transformer. Hence the generator effi-
ciency is enhanced, and the generator weight and volume are reduced. Semiconductor devices
are employed in the circuit and thus it can be considered as a cost-effective, high-voltage pulse
generator. The cascaded boost converter has better voltage gain than a single-stage boost converter
and also works in continuous current mode. The combination of the cascaded boost converter
and high-voltage pulse generator proves better impedance matching. Also, the proper impedance
matching is required to avoid the load change reflection on the input battery side. The circuit reli-
ability is improved for different switching frequencies and a duty ratio. The number of MOSFETs
included in the high-voltage pulse generator can be increased to raise the voltage magnitude and
to reduce the voltage stress on each individual MOSFET. However, care must be taken to use a
well-synchronized driver circuit to trigger individual MOSFETs.

References

[1] Nazni P., Shobana Devi R., *Effect of Processing on the Characteristics Changes in Barnyard and
    Foxtail Millet*, Journal of Food Processing Technology, vol. 7, no. 3, pp. 1–8 (2016).

[2] Khanam A., Platel K., *Influence of domestic processing on the bioaccessibility of selenium from selected food grains and composite meals*, Journal of Food Science and Technology, vol. 53, no. 3, pp. 1634–1639 (2016).

[3] Gabaza M., Shumoy H., Louwagie L., Muchuweti M., Vandamme P., Du Laing G., Raes K., *Traditional fermentation and cooking of finger millet: Implications on mineral binders and subsequent bioaccessibility*, Journal of Food Composition and Analysis, vol. 68, pp. 87–94 (2018).

[4] Sunil Neelash C., Jaivir S., Suresh C., Vipul C., Vikrant K., *Non-thermal techniques: Application in food industries-A review*, Journal of Pharmacognosy and Phytochemistry, vol. 7, no. 5, pp. 1507–1518 (2018).

[5] Nowosad K., Sujka M., Pankiewicz U., Kowalski R., *The application of PEF technology in food processing and human nutrition*, Journal of Food Science and Technology, vol. 58, pp. 397–411 (2020), DOI: 10.1007/s13197-020-04512-4.

[6] Rana Muhammad A., Xin-An Z., Zhong H., Amna S., Anees Ahmed K., Ubaid U.R., Muneeb K., Tariq M., *Combined effects of pulsed electric field and ultrasound on bioactive compounds and microbial quality of grapefruit juice*, Journal of Food Processing and Preservation, vol. 42, no. 2 (2018), DOI: 10.1111/jfpp.13507 (2018).

[7] Ramune B., Gianpiero P., Nerijus L., Saulius S., Pranas V., Giovanna F., *Application of pulsed electric field in the production of juice and extraction of bioactive compounds from blueberry fruits and their by-products*, Journal of Food Science and Technology, vol. 52, no. 9, pp. 5898–5905 (2015).

[8] Carbonell-Capella J.M., Buniowska M., Cortes C., Zulueta A., Frigola A., Esteve M.J., *Influence of pulsed electric field processing on the quality of fruit juice beverages sweetened with Stevia rebaudiana*, Food and Bioproducts Processing, vol. 101, pp. 214–222 (2017).

[9] Caminity I.M., Palgan I., Noci F., Arantxa Muñoz, Whyte P., Cronin D.A., Morgan D.J., Lyng J.G., *The effect of pulsed electric fields (PEF) in combination with high intensity light pulses (HILP) on Escherichia coli inactivation and quality attributes in apple juice*, Innovative Food Science and Emerging, vol. 12, no. 2, pp. 118–123 (2011).

[10] Morales-de la Pena M., Elez-Martinez P., Martin-Belloso O., *Food Preservation by Pulsed Electric Fields: An Engineering Perspective*, Food Engineering Reviews, vol. 3, pp. 94–107 (2011).

[11] Buckow R., Sieh N., Toepfl S., *Pulsed electric field processing of orange juice: a review on microbial, enzymatic, nutritional and sensory quality and stability*, Comprehensive Reviews in Food Science and Food safety, vol. 12, pp. 455–467 (2013).

[12] Toepfl S., *Pulsed electric field food processing – Industrial equipment design and commercial applications*, Stewart Postharvest Review, vol. 8, pp. 1–7 (2012).

[13] Valic B., Muriel Golzio, Mojca Pavlin, Anne Schatz, Cecile Faurie, Weaver J.C., *Electroporation of Cells and Tissues*, IEEE Transaction on Plasma Science, vol. 28, pp. 24–33 (2000).

[14] Toepfl S., Heinz V., Knorr D., *High intensity pulsed electric fields applied for food preservation*, Chemical Engineering and Processing, vol. 46, pp. 537–546 (2007).

[15] Geveke D.J., Kozempel M., Scullen O.J., Brunkhorst C., *Radio frequency energy effects on microorganisms in foods*, Innovative Food Science and Emerging Technology, vol. 3, no. 2, pp. 133–138 (2002).

[16] Geveke D.J., Brunkhorst C., *Inactivation of Escherichia coli in apple juice by radio frequency electric fields*, Journal of Food Science, vol. 69, pp. 134–138 (2004).

[17] Geveke D.J., Brunkhorst C., Fan X., *Radio frequency electric fields processing of orange juice*, Innovative Food Science and Emerging Technologies, vol. 8, pp. 549–554 (2007).

[18] Krishnaveni S., Rajini V., *Diode clamped gate driver-based high voltage pulse generator for electro-poration*, Turkish Journal of Electrical Engineering and Computer Sciences, vol. 26, pp. 2374–2384 (2018).

[19] Pokryvailo A., Yankelevich Y., Shapira M., *A compact source of sub gigawatt sub-nanosecond pulses*, IEEE Transaction on Plasma Science, vol. 32, pp. 1909–1918 (2004).

[20] Wu Y., Liu K., Qiu J., X., Xiao H., *Repetitive and high voltage Marx generator using solid-state devices*, IEEE Transaction on Dielectrics and Electrical Insulation, vol. 14, pp. 937–940 (2007).

[21] Ramya R., Raja P.R., Gowrisree V., *High Voltage Pulsed Electric Field Application Using Titanium Electrodes for Bacterial Inactivation in Unpurified Water*, Japan Journal of Food Engineering, vol. 20, no. 2, pp. 63–70 (2019).

[22] Kasri N.N.F., Piah M.A.M., Adzis Z., *Compact High-Voltage Pulse Generator for Pulsed Electric Field Applications: Lab-Scale Development*, Journal of Electrical and Computer Engineering, vol. 2020, art. ID 6525483, pp. 1–12 (2020), DOI: 10.1155/2020/6525483.

[23] Flisara K., Meglica S.H., Morelj J., Golobb J., Miklavcic D., *Testing a prototype pulse generator for a continuous flow system and its use for E. coli inactivation and microalgae lipid extraction*, Bioelectochemistry, vol. 100, pp. 44–51 (2014).

[24] Merensky L.M., Kardo-Sysoev A., Shmilovitz D., Kesar A.S., *Efficiency Study of a 2.2 kV, 1 ns, 1 MHz Pulsed Power Generator Based on a Drift-Step-Recovery Diode*, IEEE Transactions on Plasma Science, vol. 41, no. 11, pp. 3138–3142 (2013).

[25] Zhang Y., Liu J., Cheng X., Zhang H., Bai G., *A Way for High-Voltage μs-Range Square Pulse Generation*, IEEE Transactions on Plasma Science, vol. 39, no. 4, pp. 1125–1130 (2011).

[26] Merla C., Amari S.E., Kenaan M., Liberti M., Apollonio F., Arnaud-Cormos D., Couder V., *A 10-Ω High-Voltage Nanosecond Pulse Generator*, IEEE Transactions on Microwave Theory and Techniques, vol. 58, no. 12, pp. 4079–4085 (2010).

[27] Ndtoungou A., Hamadi A., Missanda A., Al-Haddad K., *Modeling and control of a cascaded Boost Converter for a Battery Electric Vehicle*, IEEE Electrical Power and Energy Conference, London, ON, Canada, pp. 182–187 (2012).

[28] Stala R., Pirog S., *DC–DC boost converter with high voltage gain and a low number of switches in multisection switched capacitor topology*, Archives of Electrical Engineering, vol. 67, no. 3, pp. 617–627 (2018), DOI: 10.24425/123667.

[29] Chen Z., Yong W., Gao W., *PI and Sliding Mode Control of a Multi-Input-Multi-Output Boost-Boost Converter*, WSEAS Transactions on Power Systems, vol. 9, pp. 87–102 (2014).

[30] Sira-Ramirez H., Silva-Origoza R., *Control design techniques in power electronics devices*, Springer (2006).

[31] Aamir M., Shinwari M.Y., *Design, implementation and experimental analysis of two-stage boost converter for grid connected photovoltaic system*, 3rd IEEE International Conference on Computer Science and Information Technology, Chengdu, China, pp. 194–199 (2010).

[32] Park S., Choi S., *Soft-switched CCM boost converters with high voltage gain for high power applications*, IEEE Transaction on Power Electronics, vol. 25, no. 5, pp. 1211–1217 (2010).

[33] Silveira G.C., Tofoli F.L., Bezerra L.D.S., Torrico-Bascope R.P., *A nonisolated DC-DC boost converter with high voltage gain and balanced output voltage*, IEEE Transaction on Industrial Electronics, vol. 61, no. 12, pp. 6739–6746 (2014).

[34] Sanders J.M., Kuthi A., Wu., Y.H., Vernier P.T., Gundersen M.A., *A linear, single-stage, nanosecond pulse generator for delivering intense electric fields to biological loads*, IEEE Transactions on Dielectrics and Electrical Insulation, vol. 16, no. 4, pp. 1048–1054 (2009).